

# Correlation of single trapping and detrapping effects in drain and gate currents of nanoscaled nFETs and pFETs

M. Toledano-Luque<sup>1,\*</sup>, B. Kaczer<sup>1</sup>, E. Simoen<sup>1</sup>, R. Degraeve<sup>1</sup>, J. Franco<sup>1,3</sup>, Ph. J. Roussel<sup>1</sup>, T. Grasser<sup>2</sup>, G. Groeseneken<sup>1,3</sup>

<sup>1</sup>imec, Kapeldreef 78, B-3001 Leuven, Belgium.

\*Phone: +32 16 281647, toleda@imec.be

<sup>2</sup>Institute for Microelectronics, Technische Universität Wien, Gußhausstraße 27-29, A-1040 Vienna, Austria.

<sup>3</sup>Dept. Elektrotechniek ESAT-MICAS, KU Leuven, Kasteelpark Arenberg 10, B-3001 Leuven, Belgium.

**Abstract** — The correlation of discrete gate and drain current fluctuations is revealed in nanoscaled SiON pFETs and nFETs, demonstrating that discrete trapping and detrapping events in the same single states are responsible of both  $I_D$  and  $I_G$  random telegraph noise (RTN). The high and low gate current  $I_G$ -RTN levels are independent of temperature but the switching rates are thermally activated indicating that the trapping and detrapping events are consistent with nonradiative multiphonon theory.

**Index Terms** — Random Telegraph Noise RTN, Gate current RTN,  $I_G$ -RTN, drain current RTN,  $I_D$ -RTN, gate leakage current, MOSFET, reliability, variability, SiON.

## I. INTRODUCTION

As a consequence of the reduction of both the gate oxide thickness and the lateral dimensions of the CMOS devices, the amount of oxide defects has decreased to a numerable level, allowing the decoupling of their collective behavior. In ultra thin gate oxide field effect transistors (FETs), discrete fluctuations of the gate leakage current are distinguishable [1], resulting in significant time-dependent variations in this important FET parameter. Likewise, in nanoscaled FETs, drain current fluctuations at inversion conditions have been recurrently reported and ascribed to trapping and detrapping events in the gate oxide [2-3].

Recently, discrete increases of the drain current, i.e. drops of the threshold voltage  $V_{TH}$ , in nanoscaled devices after gate bias temperature (BTI) stress have been seen in nFETs and pFETs with SiON and high- $\kappa$  dielectrics and have been explained by the discharge of individual traps [4-9]. This effect has been described as the non-steady state case of the drain random telegraph noise  $I_D$ -RTN [4] (Fig. 1).

The correlation between the fluctuations in the drain current  $I_D$ -RTN and the gate current  $I_G$ -RTN has been pointed out by Chen *et al.* [10] for nFET devices. In this paper, we further explore the  $I_D$ -RTN and  $I_G$ -RTN correlation, not only for nFETs but also for pFETs, demonstrating that both effects are due to the charging and

discharging of the same isolated defects. Consequently, we argue that the same states play a fundamental role in the two major reliability issues of CMOS technology: the threshold voltage instability and the gate leakage current (Fig. 1).

## II. DEVICES AND EXPERIMENTAL SETUP

The transfer characteristics ( $I_D$  vs.  $V_G$ ) and leakage current curves ( $I_G$  vs.  $V_G$ ) were registered in different SiON pFETs and nFETs by means of Keithley 2636 SMUs. Afterward,  $I_D$  and  $I_G$  traces were simultaneously measured with a sample rate of 20ms at a target absolute gate current of 10pA. The transient characteristics of a selected nFET and a pFET were measured additionally at different gate voltages and temperatures ranging from 15 to 65°C. The drain voltage  $V_D$  was fixed to 1100mV during all the characterizations.

The experimental  $V_G$  window that allows measuring simultaneously  $I_D$ -RTN and  $I_G$ -RTN is limited to a relatively narrow interval. This is because the largest  $I_D$ -RTN fluctuations with respect to  $I_D$  are observed at low  $V_G$  (close to  $V_{TH}$ ) but  $I_G$ -RTN amplitude increases with  $V_G$ . This point

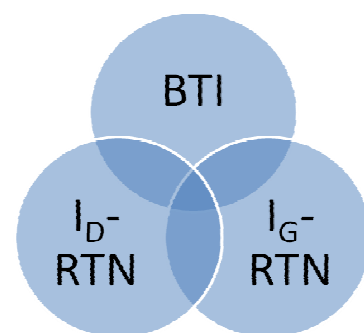


**Fig. 1:** Same states are argued to be responsible for the threshold voltage  $V_{TH}$  instabilities observed at stationary and dynamic bias conditions ( $I_D$ -RTN and BTI, respectively) [4] and the leakage current  $I_G$  fluctuations ( $I_G$ -RTN).

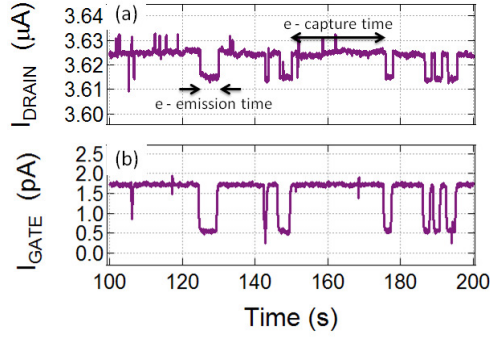


**Fig. 2:** (a)  $I_D$  and (b)  $I_G$  traces simultaneously registered by means of Keithley 2636 SMUs on a nanoscaled  $90 \times 35 \text{ nm}^2$  2.3nm-EOT SiON nFET showing synchronized fluctuations and demonstrating the correlation between  $I_D$  and  $I_G$  RTN. The lower level of the drain current corresponds to the periods when the trap is negatively charged. Therefore, the emission and the capture times are obtained from the periods when the current is at low and high levels, respectively.

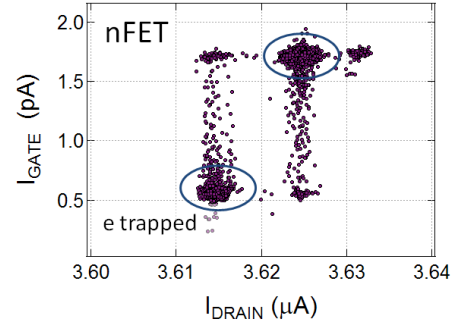


**Fig. 4:** Gate current  $I_G$  vs. drain current  $I_D$  from Fig. 2 for fixed sampling times. The correlation between both variables becomes more evident. The high  $I_G$  level corresponds to the high  $I_D$  value. The events registered outside of the expected clusters are due to the mismatch in the synchronization of the measured currents at the two terminals.

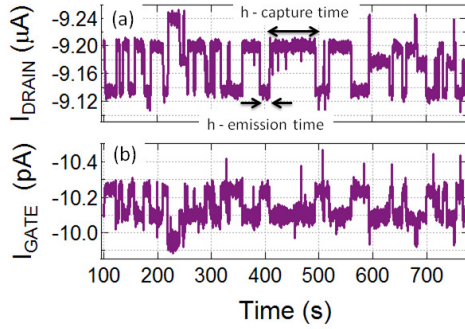


**Fig. 3:** The correlation between (a)  $I_D$  and (b)  $I_G$  RTN is also shown for SiON pFETs. However, it is observed that the high  $I_G$  level corresponds to the low  $I_D$  value. The low level of the drain current corresponds to the periods when a hole is trapped. The emission and capture times are obtained from the periods when the drain current is at low and high values, respectively.

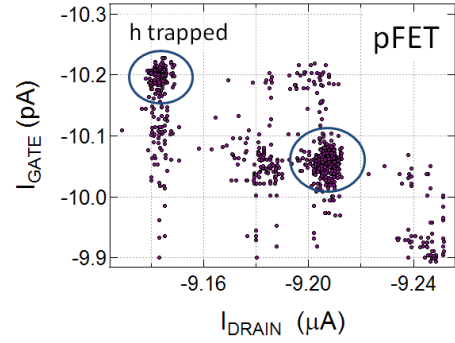


**Fig. 5:** Inverse correlation between  $I_D$  and  $I_G$  is found for the pFET (Fig. 3) with respect to the nFET case (see Fig. 4). The high  $I_G$  level corresponds to a low  $I_D$  value.

is extended later on.

Nanoscaled devices with an area of  $W \times L = 70 \times 35 \text{ nm}^2$  were studied. 2.3nm-EOT SiON pFETs and nFETs were selected because they fulfill two essential requirements for this experiment: significant leakage current with a sufficient EOT.

- (1) The thick EOT ensures high average  $I_D$ -RTN amplitude since  $\Delta I_D$  is approximately proportional to the EOT of the stack [11-13]. So the thicker the gate oxide is, the larger the average  $I_D$ -RTN amplitude gets.
- (2) However, the leakage current  $I_G$  decays exponentially with increasing the physical thickness of gate oxide. Therefore, thin oxides are mandatory to observe a sufficient gate current with our experimental setup.

### III. CORRELATION OF DRAIN AND GATE CURRENT RANDOM TELEGRAPH NOISES

Figures 2 and 3 show the  $I_G$  and  $I_D$  traces registered in parallel for a representative nFET and pFET, respectively. An evident correlation of  $I_G$ -RTN and  $I_D$ -RTN is observed for both cases. For the nFET, a high drain current level corresponds to a high gate current level. However, the correlation is inverted for the pFET, a high drain current level corresponds to a low gate current level. The correlation between  $I_D$  and  $I_G$  fluctuations is more evident in Figs. 4 and 5 where the gate current  $I_G$  is plotted vs. the drain current  $I_D$  at each measured time-stamp. Note that two main clusters appear in the graphs. The events registered outside of the expected clusters are due to the mismatch in the synchronization of the measured currents at the two terminals.

Figs. 2 and 3 also show that the absolute value of the drain current fluctuations  $\Delta I_D$  is orders of magnitude larger than the  $I_G$ -RTN amplitude  $\Delta I_G$ . Therefore, no direct conduction paths are formed between the gate and the source/drain terminals as it is the case of  $I_D$ -RTN and  $I_G$ -RTN after soft breakdown or in RRAM filaments inside a transistor [14-16].

The large  $I_D$ -RTN signals observed in Figs. 2 and 3 are due to the non-uniform potential at the Si/SiON interface caused by the random distributions of dopants in the channel and charged traps in the dielectric, as illustrated in Fig. 6. The potential fluctuations produce variations of the inversion charge density and, consequently, preferential conduction paths from the drain to the source. The charge and discharge of single oxide traps over critical positions of the conduction paths can produce significant fluctuations of the drain current

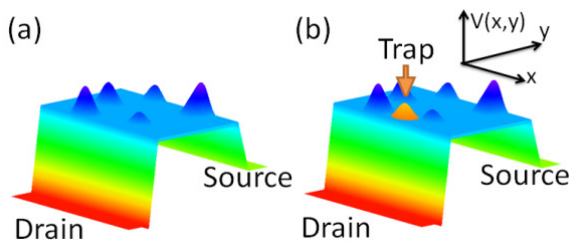


**Fig. 6:** (a) Percolation paths are formed between the drain and the source in a nanoscaled device due to potential fluctuations caused by random dopant distribution and charged gate oxide traps. (b) An additional charged trap may block a percolation path, causing a significant decrease of  $I_D$ .

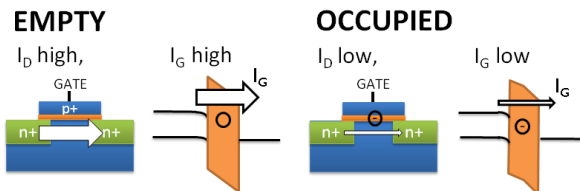


**Fig. 7:** According to the model presented in [14,15], *electron trapping* in the gate oxide of a nFET may cause a significant drop of  $I_D$  electron current and a simultaneous *raise of the oxide conduction band*, reducing the electron tunneling probability and therefore the gate leakage current.

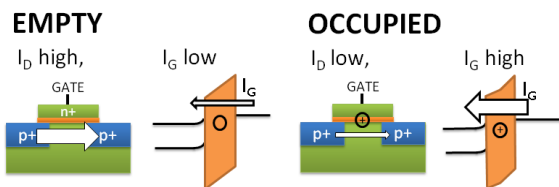


**Fig. 8:** *Hole trapping* in the gate oxide of a pFET may also cause a significant drop of  $I_D$  hole current and a simultaneous *lowering of the oxide conduction band* thus increasing the electron tunneling probability and therefore the gate leakage current [14,17].

[11-12]. On the other hand, the  $I_G$  fluctuations may be explained either by (1) the local increase/decrease of the electron tunneling barrier [14,17] produced by an electron/hole trapped in the dielectric, as illustrated in Figs. 7 and 8 or by (2) trap assisted tunneling through defects with two possible states and, therefore, two possible pairs of emission and capture times [18-19].

- (1) For the nFET in Figs. 2 and 4, the lower  $I_D$  level corresponds to the case of an electron trapped in the dielectric, and a sudden increase of the current is detected at the very moment that the electron is emitted. Figs. 2 and 4 show an important decrease of the leakage current when the electron is trapped. A higher leakage current is detected when the trap is discharged.

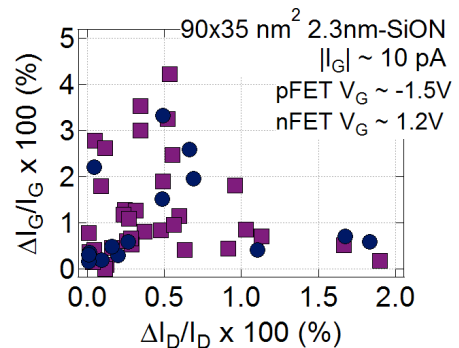


**Fig. 9:** No obvious correlation is found between the  $I_G$ -RTN and  $I_D$ -RTN amplitudes for nFETs or pFETs showing simultaneous  $I_G$  and  $I_D$  RTN. Low  $\Delta I_D/I_D$  ratios are measured due to the large  $V_G$  used in the measurement (see Fig. 10).

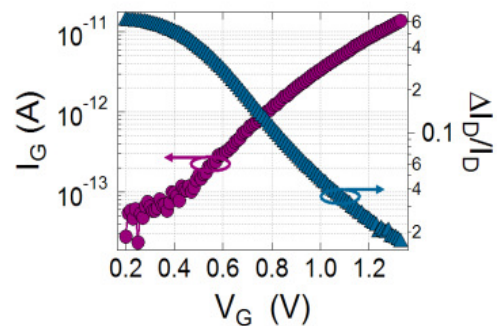


**Fig. 10:** (Left axis) Leakage current  $I_G$  and (right axis)  $\Delta I_D/I_D$  for one of the 2.3nm-EOT SiON nFETs under study as a function of the gate voltage  $V_G$ . The  $\Delta I_D/I_D$  curve is obtained by considering a constant threshold voltage shift  $\Delta V_{TH}$  of 40mV in the entire  $V_G$  range. High gate voltages are mandatory to measure a reasonable gate current  $I_G$  (left axis). However,  $I_D$ -RTN sensitivity (right axis) is reduced at high gate voltages. Consequently, simultaneous measurement of  $I_D$ -RTN and  $I_G$ -RTN is limited to a relatively narrow  $V_G$  window.

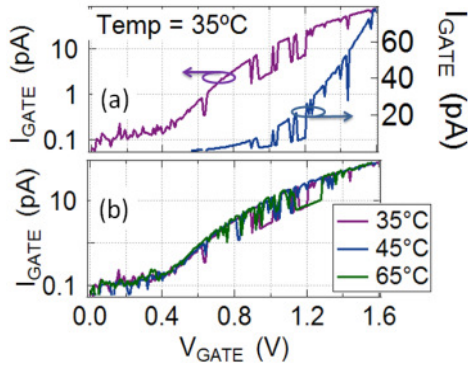


**Fig. 11:** (a) Charge and discharge processes are visible in the  $I_G$ - $V_G$  curve. The vertical shift of the low and high  $I_G$  levels in log scale indicates a constant ratio between the two levels. (b) No thermal dependence of the high and low  $I_G$  envelopes is observed. However,  $I_G$  current is modulated by a thermally activated process of trapping/detrapping of charge.

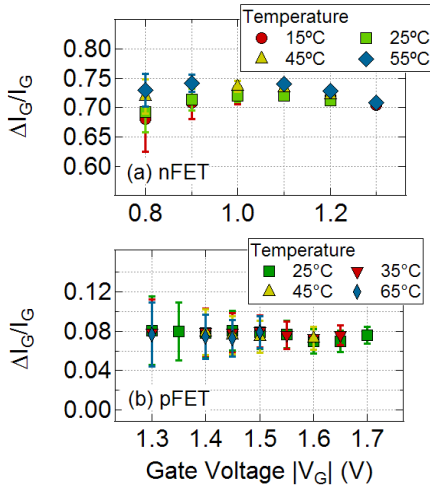


**Fig. 12:** Relative gate current RTN ( $\Delta I_G/I_G$ ) amplitude as a function of gate voltage  $V_G$  at different temperatures for (a) the same nFET as shown in Fig. 11 and (b) for a pFET.

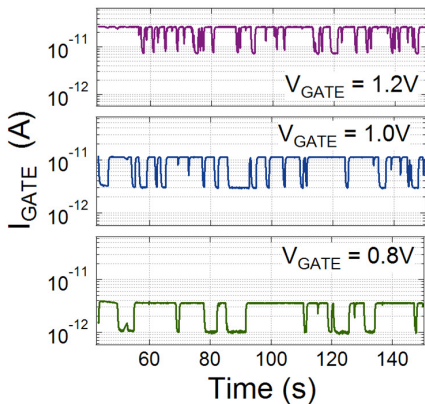


**Fig. 13:** High-to-low  $I_G$  ratio is constant in the range of scanned  $V_G$ , but emission and capture processes become more frequent with increasing  $V_G$  for the trap observed at Fig. 11.

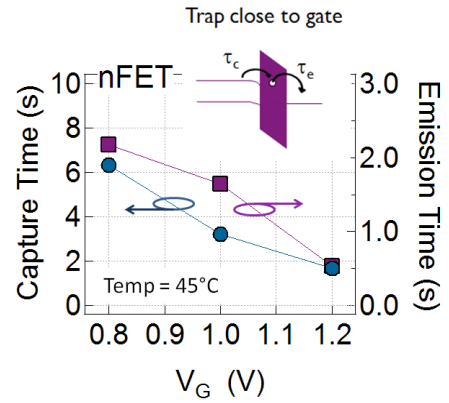


**Fig. 14:** Capture  $\tau_c$  and emission  $\tau_e$  times extracted at different  $V_G$ 's for the nFET shown in Fig. 13. For this particular case, a decrease of  $\tau_c$  is observed with  $V_G$  increasing. Conversely to NBTI experiments [20],  $\tau_e$  decreases with  $V_G$ . This trend suggests the possibility of charge exchange also with the gate as sketched in inset.

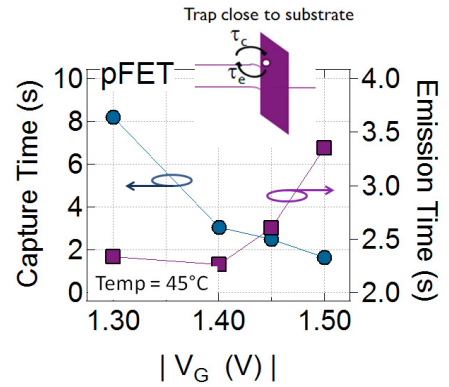


**Fig. 15:**  $\tau_c$  and  $\tau_e$  follow the same trend as NBTI experiments [20-21], hinting at charge exchange with the substrate.

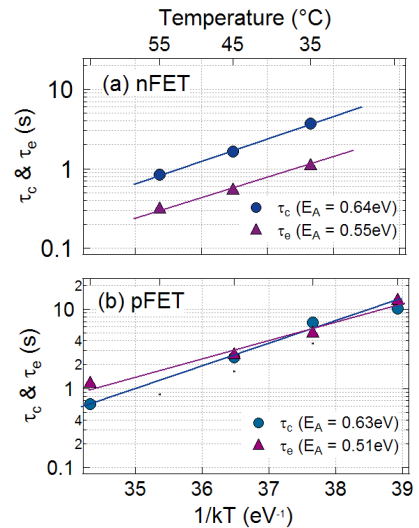


**Fig. 16:** Arrhenius plots of the emission  $\tau_e$  and capture  $\tau_c$  times for (a) an nFET at  $V_G = 1.2\text{V}$  and (b) a pFET at  $V_G = -1.45\text{V}$  show a strong temperature dependence of both parameters.

- (2) For the pFET in Figs. 3 and 5, the inverse trend is observed: an  $I_D$  reduction (a hole capture) corresponds to an enlargement of  $I_G$ . Therefore the high level of leakage current is detected when the trap is positively charged as sketched in Fig. 8.

Therefore, the reverse correlation between  $I_G$ -RTN and  $I_D$ -RTN in nFETs and pFETs arises from the fact that the gate current is due to electron carriers, while the drain current is hole current for pFETs and electron current for nFETs.

At an  $|I_G|$  of about 10pA, the correlation between  $I_D$ -RTN and  $I_G$ -RTN fluctuations was corroborated on 37 out of 235 pFETs and on 18 out of 308 nFETs. Fig. 9 shows the relative amplitude of the gate current RTN and drain current RTN for the devices showing simultaneously both effects. Although the number of analyzed devices is limited, the absence of devices showing simultaneously giant  $I_G$ -RTN and giant  $I_D$ -RTN is noted and, also, an approximately reciprocal relation between the amplitudes can be discerned. However, a larger sample size is necessary to draw definite conclusions.

In Fig. 9 it is also noted that  $\Delta I_D/I_D$  is lower than  $\Delta I_G/I_G$ . This is due to the high  $V_G$  used as the sense voltage.  $\Delta I_D/I_D$  reaches its maximum at low  $V_G$  values, provided that a single charge produces a constant  $V_{TH}$  shift over the entire  $V_G$  range (Fig. 10). In this experiment, however a high sense gate voltage  $V_G$  is used in order to obtain a reasonable gate current, resulting in a reduced  $\Delta I_D/I_D$  ratio. On the other hand, the  $\Delta I_G/I_G$  is constant in the entire  $V_G$  range, as observed in Fig. 11 and discussed in the next section. Therefore, it is feasible to observe  $I_D$ -RTN at low  $V_G$  and  $I_G$ -RTN at high  $V_G$ , limiting the possibility of simultaneously recording both effects to a narrow  $V_G$  window.

#### IV. GATE CURRENT RTN

Figure 11 shows the  $I_G$  vs.  $V_G$  curves at different temperatures of a device showing giant gate current RTN. In Fig. 11, the charge and discharge processes are clearly observed during  $I_G$ - $V_G$  tracing. Note that the high and low  $I_G$  levels are independent of temperature. The constant vertical shift between the low  $I_G$  and high  $I_G$  when plotted on a log scale, see Fig. 11(b), suggests a constant ratio between the two levels over the entire scanned  $V_G$  range. In order to further document this fact, Fig. 12(a) shows the relative amplitude  $\Delta I_G/I_G$  as a function of gate voltage  $V_G$  for different temperatures. An approximately constant  $\Delta I_G/I_G$  ratio is observed. These results, temperature independent gate current and constant  $\Delta I_G$  ratio were also observed for the trap studied in a selected pFET device. Fig. 12(b) shows that the  $\Delta I_G/I_G$  ratio is constant and independent of temperature and gate voltage. These facts are in agreement with both the charge blocking area model [14, 17] and the two state defect approach [18-19].

Fig. 13 shows the  $I_G$  traces registered on the same device as in Fig. 11 for different  $V_G$ 's. A higher probability of emission and capture of charge, i.e. shorter capture  $\tau_c$  and emission  $\tau_e$  times, is observed with increasing  $V_G$  for the single trap under study. The emission and capture times are stochastic variables that follow an exponential distribution

(not shown) [3]. This exponential distribution for the emission and capture times has been also reported for  $I_D$ -RTN and BTI experiments on nanoscaled devices [20-21]. Fig. 14 shows the average values of the emission  $\tau_e$  and capture times  $\tau_c$  obtained as a function of the gate voltage  $V_G$  from the traces presented in Fig. 13. As expected  $\tau_c$  decreases with  $V_G$ , thus, the capture probability increases. Interestingly,  $\tau_e$  also decreases. This may point to electron capture from the silicon channel and emission into the polysilicon gate, as depicted in the inset of Fig. 14. Fig. 15 shows the  $\tau_c$  and  $\tau_e$  values as a function of  $V_G$  for a trap in a pFET. In this case, the capture time decreases with increasing the gate voltage and the emission time increases. This is the expected BTI behavior: reduction of  $\tau_c$  and increase of  $\tau_e$  with increasing  $V_G$  [20-21].

These different behaviors suggest the possibility of charge exchange not solely with the silicon channel (inset of Fig. 15) as assumed in BTI experiments, but also with the polysilicon gate (inset of Fig. 14). It may indicate that  $V_{TH}$  shifts observed in TDDS experiments [20] are due to traps placed close to the silicon interface, where the probability of charge emission to the gate is limited even at high (stress) gate voltages.

The *thermal activation of the charging and discharging* processes is demonstrated by repeating the experiment at different temperatures. Fig. 16 shows the Arrhenius plot of the capture and emission times for the traps in Figs. 14 and 15. For temperatures above 55 and 65°C the characteristic times for the traps in the nFET and the pFET, respectively, drop below the 1 second range, making the extraction of the emission and capture times difficult (the sampling time of our setup is 20ms). Activation energies  $E_A$  of about 0.6eV are extracted for the capture and the emission times. These large activation energies disagree again with the elastic tunneling theory extensively used for trapping/detrapping processes in the operation model of charge trap memories [22], spatial depth profiling [23], and  $I_D$ -RTN [24]. Moreover, these energies are similar to the ones obtained in BTI experiments on nanoscaled devices [5-7, 20-21]. We therefore conclude that the same traps are responsible for both effects, but traps placed closer to the gate present a higher probability of being emptied during stress, thus, not contributing to BTI.

#### V. CONCLUSIONS

In conclusion, the one-to-one correlation between  $I_G$ -RTN and  $I_D$ -RTN has been shown for both nFETs and pFETs. This correlation demonstrates that the same traps are responsible for both effects. Gate leakage current is modulated by a thermally activated process of trapping and detrapping of charge.  $I_G$ -RTN can be extremely useful as a fast technique to gather information on dielectric traps in ultra low EOT gate oxide capacitors without the necessity of full transistor processing.

#### VI. ACKNOWLEDGMENTS

This work was performed as part of imec's Core Partner Program. It has been in part supported by the European Commission under the 7th Framework Programme (Collaborative project MORDRED, contract No. 261868).



## REFERENCES

- [1] R. Degraeve, T. Kauerauf, M. Cho, M. Zahid, L.Å. Ragnarsson, D.P. Brunco, B. Kaczer, Ph. Roussel, S. De Gendt, G. Groeseneken, "Degradation and breakdown of 0.9 nm EOT SiO<sub>2</sub>/ALD-HfO<sub>2</sub>/metal gate stacks under positive constant voltage stress," in *Electron Devices Meeting, 2005. IEDM Technical Digest. IEEE International*, pp. 408-411, Dec. 2005.
- [2] K.S. Ralls, W.J. Skocpol, L.D. Jackel, R.E. Howard, L.A. Fetter, R.W. Epworth, D.M. Tennant, "Discrete Resistance Switching in Submicrometer Silicon Inversion Layers: Individual Interface Traps and Low-Frequency (1/f?) Noise," *Phys. Rev. Lett.*, vol. 52, no. 3, pp. 228-231, Jan. 1984.
- [3] E. Simoen, B. Kaczer, M. Toledano-Luque, and C. Claeys, "Random telegraph noise: from a device physicist's dream to a designer's nightmare," *ECS Trans.* vol. 39, no. 3, pp. 3-15, Sept. 2011.
- [4] B. Kaczer, T. Grasser, J. Martin-Martinez, E. Simoen, M. Aoulaiche, Ph.J.Roussel, G. Groeseneken, "NBTI from the perspective of defect states with widely distributed time scales," in *Reliability Physics Symposium, 2009 IEEE International*, pp. 55-60, April 2009.
- [5] T. Grasser, H. Reisinger, P. Wagner, F. Schanovsky, W. Goes, B. Kaczer, "The time dependent defect spectroscopy (TDDS) for the characterization of the bias temperature instability," in *Reliability Physics Symposium (IRPS), 2010 IEEE International*, pp. 16-25, May 2010.
- [6] M. Toledano-Luque, B. Kaczer, Ph.J. Roussel, M.J. Cho, T. Grasser, G. Groeseneken, "Temperature dependence of the emission and capture times of SiON individual traps after positive bias temperature stress," *Journal of Vacuum Science & Technology B: Microelectronics and Nanometer Structures*, vol. 29, no.1, pp.01AA04-01AA04-5, Jan 2011.
- [7] M. Toledano-Luque, B. Kaczer, E. Simoen, Ph. J. Roussel, A. Veloso, T. Grasser, G. Groeseneken, "Temperature and voltage dependences of the capture and emission times of individual traps in high-k dielectrics," *Microelectronic Engineering*, vol. 88, no. 7, pp. 1243-1246, July 2011.
- [8] C.-T. Chan, C.-J. Tang, T.Wang, H. C.-H.Wang, and D. D. Tang, "Characteristics and physical mechanisms of positive bias and temperature stress-induced drain current degradation in HfSiON nMOSFETs," *IEEE Trans.Electron Devices*, vol. 53, no. 6, pp. 1340-1346, Jun. 2006.
- [9] V. Huard, C. Parthasarathy, C. Guerin, T. Valentin, E. Pion, M. Mammasse, N. Planes, L. Camus, "NBTI degradation: From transistor to SRAM arrays," *Reliability Physics Symposium, 2008. IRPS 2008. IEEE International*, pp.289-300, May 2008.
- [10] C. Chia-Yu, R. Qiushi, C. Hyun-Jin, A. Kerber, L. Yang, L. Ming-Ren, R.W. Dutton, "Correlation of I<sub>d</sub>- and I<sub>g</sub>-random telegraph noise to positive bias temperature instability in scaled high-κ/metal gate n-type MOSFETs," in *Reliability Physics Symposium (IRPS), 2011 IEEE International*, pp. 3A.2.1-3A.2.6, April 2011.
- [11] A. Ghetti, C.M. Compagnoni, A.S. Spinelli, A. Visconti, "Comprehensive analysis of Random Telegraph Noise instability and its scaling in deca-nanometer Flash memories," *Electron Devices, IEEE Transactions on*, vol. 56, no. 8, pp.1746-1752, Aug. 2009.
- [12] A. Asenov, R. Balasubramaniam, A.R. Brown, J.H. Davies, "RTS amplitudes in decanometer MOSFETs: 3-D simulation study," *Electron Devices, IEEE Transactions on*, vol. 50, no. 3, pp. 839- 845, March 2003.
- [13] M. Toledano-Luque, B. Kaczer, Ph. J. Roussel, J. Franco, L. Å. Ragnarsson, T. Grasser, and G. Groeseneken, "Depth localization of positive charge trapped in silicon oxynitride field effect transistors after positive and negative gate bias temperature stress," *Appl Phys. Lett.*, vol. 98, no. 18, pp. 183506, May 2011.
- [14] F. Crupi, G. Giusi, G. Iannaccone, P. Magnone, C. Pace, E. Simoen, C. Claeys, "Analytical model for the 1/f noise in the tunneling current through metal-oxide-semiconductor structures," *Journal of Applied Physics*, vol. 106, no. 7, pp. 073710-073710-6, Oct 2009.
- [15] R. Degraeve, L. Goux, Ph. Roussel, D.J. Wouters, J.A. Kittl, L. Altissime, M. Jurczak, G. Groeseneken, "Deterministic and stochastic component in RESET transient of HfSiO/FUSI gate RRAM stack," in *VLSI Technology (VLSIT), 2011 Symposium on*, pp.28-29, 14-16 June 2011.
- [16] D. Ielmini, F. Nardi, C. Cagli, "Resistance-dependent amplitude of random telegraph signal noise in resistive switching memories," *Appl Phys. Lett.*, vol. 96, no. 5, pp. 053 503, Feb. 2010.
- [17] R. Degraeve, "Time dependent dielectric breakdown in thin oxides: mechanisms, statistics and oxide reliability prediction," *PhD dissertation*, K.U. Leuven, 1998.
- [18] M. O. Andersson, Z. Xiao, S. Norrman, O. Engstrom, "Model based on trap-assisted tunneling for two-level current fluctuations in submicrometer metal/silicon-dioxide/silicon diodes," *Phys. Rev. B*, vol. 41, no. 14, pp. 9836, May 1990.
- [19] T. Grasser, B. Kaczer, H. Reisinger, P.-J. Wagner, M. Toledano-Luque, "On the frequency dependence of the Bias Temperature Instability," in *Reliability Physics Symposium (IRPS), 2012 IEEE International*, April 2012.
- [20] T. Grasser, H. Reisinger, P.-J. Wagner, B. Kaczer, "Time-dependent defect spectroscopy for characterization of border traps in metal-oxide-semiconductor transistors," *Phys. Rev. B* vol. 82, no. 24, pp. 245318-245318, Dec. 2010.
- [21] M. Toledano-Luque, B. Kaczer, Ph.J. Roussel, T. Grasser, G.L. Wirth, J. Franco, C. Vrancken, N. Horiguchi, G. Groeseneken, "Response of a single trap to AC negative Bias Temperature stress," in *Reliability Physics Symposium (IRPS), 2011 IEEE International*, pp. 4A.2.1-4A.2.8, April 2011.
- [22] E. Vianello, L. Perniola, P. Blaise, G. Molas, J.P. Colonna, F. Driussi, P. Palestri, D. Esseni, L. Selmi, N. Rochat, C. Licitra, D. Lafond, R. Kies, G. Reimbold, B. De Salvo, F. Boulanger, "New insight on the charge trapping mechanisms of SiN-based memory by atomistic simulations and electrical modeling," in *Electron Devices Meeting (IEDM), 2009 IEEE International*, pp.1-4, Dec. 2009.
- [23] R. Degraeve, M. Cho, B. Govoreanu, B. Kaczer, M.B. Zahid, J. Van Houdt, M. Jurczak, G. Groeseneken, "Trap Spectroscopy by Charge Injection and Sensing (TSCIS): A quantitative electrical technique for studying defects in dielectric stacks," in *Electron Devices Meeting, 2008. IEDM 2008. IEEE International*, pp. 1-4, Dec. 2008.
- [24] T. Nagumo, K. Takeuchi, T. Hase, Y. Hayashi, "Statistical characterization of trap position, energy, amplitude and time constants by RTN measurement of multiple individual traps", in *Electron Devices Meeting, 2008. IEDM 2010. IEEE International*, pp. 28.3.1-28.3.4, Dec. 2010.